Carbohydrate Polymers 86 (2011) 1665–1670

Contents lists available at ScienceDirect

Carbohydrate Polymers

journal homepage: www.elsevier.com/locate/carbpol

Self-assembled nanoparticles of methotrexate conjugated *O*-carboxymethyl chitosan: Preparation, characterization and drug release behavior *in vitro*

Yinsong Wang[a,b,*], Xiaoying Yang[a], Jinrong Yang[a], Yumei Wang[a], Rou Chen[a], Jing Wu[b], Yuanyuan Liu[b], Ning Zhang[b,**]

[a] *Tianjin Key Laboratory on Technologies Enabling Development of Clinical Therapeutics and Diagnostics, School of Pharmacy, Tianjin Medical University, No. 22 Qixiangtai Road, Heping District, Tianjin 300070, PR China*

[b] *Research Center of Basic Medical Science, Tianjin Medical University, No. 22 Qixiangtai Road, Heping District, Tianjin 300070, PR China*

ARTICLE INFO

Article history:
Received 15 April 2011
Received in revised form 26 June 2011
Accepted 30 June 2011
Available online 7 July 2011

Keywords:
O-Carboxymethyl chitosan
Methotrexate
Nanoparticles
Sustained release

ABSTRACT

The conjugates of *O*-carboxymethyl chitosan (OCM-chitosan) with methotrexate (MTX) were synthesized by carbodiimide coupling and characterized by Fourier transform infrared (FTIR), proton nuclear magnetic resonance (^{1}H NMR) and ultraviolet spectroscopy (UV). OCM-chitosan-MTX conjugates had amphiphilic properties and their critical aggregation concentrations in aqueous media determined by fluorescence spectroscopy were 4.24×10^{-2}, 1.81×10^{-2} and 0.84×10^{-2} mg/mL, respectively, responding to MTX contents of 10.8%, 16.2% and 19.3%. OCM-chitosan-MTX nanoparticles prepared by the dialysis method had nearly spherical shape and their sizes were in the range of 187.2–363.5 nm. Meanwhile, their zeta potentials ranged from −8.19 mV to −3.08 mV. Drug releases of OCM-chitosan-MTX nanoparticles were studied by the dynamic dialysis method and MTX exhibited significant sustained-release behaviors in PBS buffer solutions (pH 4.0, 7.2 and 9.0), indicating that these nanoparticles had good *in vitro* stability and the potential to be used as a novel drug carrier system.

1. Introduction

Chemotherapeutic agents for the tumor treatment possess some inevitable and serious side effects such as non-specific toxicity, which limit their clinical uses. Many investigations have been attempted to decrease toxicity of antitumor agents to normal tissues by localizing cytotoxicity at tumor sites and employing water-soluble polymeric prodrugs to prolong the duration of drug activities (David, Kopeckova, Minko, Rubinstein, & Kopecek, 2004; Dvŏrák, Kopečková, & Kopeček, 1999; Li, 2002; Maeda, 2001a, 2001b; Nogusa, Yano, Okuno, Hamana, & Inoue, 1995; Putnam & Kopeček, 1995; Song, Onishi, & Nagai, 1992). Particularly, as the concept of "enhanced permeability and retention (EPR) effect" introduced, polymeric prodrugs have attracted more and more interests due to their passive tumor targeting properties (Fang, Sawa, & Maeda, 2003; Greish, Fang, Inutsuka, Nagamitsu, & Maeda, 2003; Maeda, 2001a, 2001b; Matsumura & Maeda, 1986). Nanotechnology is another effective strategy of tumor-targeting drug delivery. Polymeric nanoparticles have shown preferential accumulation at tumor sites, and therefore their usage as carriers improves efficacy and reduces side effects (Akiyoshi, Yamaguchi, & Sunamoto, 1991; Jones & Leroux, 1999; Kwon & Kataoka, 1995; Nishiyama & Kataoka, 2005; Torchilin, 2001). Recently, many novel carriers combining advantages of prodrug and nanotechnology have been investigated and some of them exhibited the promising *in vivo* properties, such as long circulation behavior and passive tumor targeting property (Aryal, Hu, & Zhang, 2010; Park et al., 2006; Son et al., 2003; Yoo, Lee, Oh, & Park, 2000; Yoo, Oh, Lee, & Park, 1999).

Chitosan, a biodegradable polysaccharide composed of primarily D-glucosamine repeating units, has many good bioproperties and some particular physiochemical characteristics, and therefore has been widely used in many biomedical applications, especially in the field of drug delivery system (Kumar, Muzzarelli, Muzzarelli, Sashiwa, & Domb, 2004). In our previous reports, several kinds of chitosan-based nanoparticles were prepared and their use as drug carriers were investigated *in vitro* and *in vivo* (Wang et al., 2008; Wang, Liu, Jiang, & Zhang, 2007; Wang, Liu, Weng, & Zhang, 2007; Yang et al., 2008). These nanoparticles had the high affinity for tumor cells and *in vitro* drug-sustained release property. However, the results of *in vivo* experiments in mice showed that the physically loaded drug in nanoparticles exhibited a rapid elimination

* Corresponding author at: Tianjin Medical University, No. 22 Qixiangtai Road, Heping District, Tianjin 300070, PR China. Tel.: +86 2223542068; fax: +86 2223542068.

** Corresponding author at: Tianjin Medical University, No. 22 Qixiangtai Road, Heping District, Tianjin 300070, PR China. Tel.: +86 2223542068; fax: +86 2223542068.

E-mail addresses: wangyinsong@tom.com (Y. Wang), nzhangchina@yahoo.com (N. Zhang).

0144-8617/$ – see front matter © 2011 Elsevier Ltd. All rights reserved.
doi:10.1016/j.carbpol.2011.06.080

from the bloodstream, probably due to the enzymatic degradation of nanoparticles and the subsequent increase of drug diffusion rate in nanoparticles. Therefore, we believed that if the drug is chemically bonded to the nanoparticle polymer matrix, namely, as the prodrug form to be loaded into nanoparticles, its releases *in vitro* and/or *in vivo* will be prolonged, thus provides sufficient time for drug reaching the tumor sites.

In this study, a novel chitosan based prodrug nanoparticle system was prepared and its stability was investigated *in vitro*. Methotrexate (MTX), as a model antitumor drug was conjugated to *O*-carboxymethyl chitosan (OCM-chitosan) by the amide linkage. This conjugate had amphiphilic property due to the both presence of hydrophilic polysaccharide backbone and hydrophobic MTX moieties in its molecule, and thus could form nanoparticles by self-assembly in aqueous media using the same method we published before (Chen et al., 2011). According to the results reported by Wu et al. (2009), the stable covalent bonding of OCM-chitosan and MTX was beneficial for the slow release of MTX, and consequently enhance therapeutic index and reduce toxicity of MTX.

2. Materials and methods

2.1. Materials

OCM-chitosan (viscosity average molecular weight: 1.0×10^5 Da; carboxymethylation degree: 72%) was synthesized by the method that we previously reported (Wang, Liu, Weng, & Zhang, 2007). MTX was supplied from Taizhou Candorly Sea Biochemical & Health Products Co., Ltd. (Zhejiang, China). 1,3-dicyclohexyl carbodiimide (DCC) and *N*-hydroxysuccinimide (NHS) were purchased from Sigma (St. Louis, MO, USA). Pyrene was obtained from Aldrich and purified by recrystallization from absolute ethanol. Dialysis membrane (molecular weight cutoff of 12–14 kDa) was the product of Millipore (Bedford, MA, USA). All other chemicals were analytical grade and were obtained from commercial sources.

2.2. Synthesis of N-hydroxysuccinimide activated methotrexate (NHS-activated MTX)

NHS-activated MTX was prepared according to the previous report (Zhang, Mao, Sun, He, & Wang, 2000). Briefly, MTX (4.5 g, 10 mmol) was mixed with DCC (2.1 g, 10 mmol) in 50 ml *N*,*N*-dimethyl formamide (DMF) and reacted for 18 h at 4 °C. Then, NHS (1.2 g, 10 mmol) and 0.5 mL pyridine were added to the above mixture and the whole mixture was stirred for 6 h at 4 °C. The precipitated dicyclohexyl urea was removed by filtration and the filtrate was evaporated under reduced pressure to obtain NHS-activated MTX.

2.3. Synthesis of O-carboxymethyl chitosan-methotrexate (OCM-chitosan-MTX) conjugates

MTX was conjugated to OCM-chitosan by a NHS-mediated reaction through the formation of amide linkage. The ratios of reactants were varied as shown in Table 1 to give OCM-chitosan-MTX-1, OCM-chitosan-MTX-2 and OCM-chitosan-MTX-3 with MTX content increasing. Briefly, for preparation of OCM-chitosan-MTX-1, OCM-chitosan (0.5 g) was dissolved in 100 mL of sodium bicarbonate solution (pH = 8.3), and a solution of NHS-activated MTX (0.5 g) in DMF (50 mL) was added drop-wise to alkaline solution of CMCS over 30 min. The mixture was reacted for 48 h at 4 °C, and the produced precipitate was filtered and washed with DMF, acetone and diethyl ether respectively to give the buff powder. This powder was dispersed in 30 mL water and exhaustively dialyzed (Millipore dialysis tube, molecular weight cut-off 12–14 kDa) against sodium bicarbonate solution (pH = 8.3) (3 L) and distilled water (3 L) for 2 days with 6 exchanges, and finally dried by freeze-drying (ALPHA1-2/LD plus, German) to obtain the buff, cotton wool-like product.

The IR spectra of OCM-chitosan and OCM-chitosan-MTX conjugates were measured on a FT-IR spectrometer (Nicolet NEXUS 470-ESP, USA) using KBr pellets. The ^{1}H NMR spectra of OCM-chitosan and OCM-chitosan-MTX conjugates were recorded on a 600 MHz spectrometer (JEOL JNM-ECP 600, Japan) for solutions of D_2O/CD_3COOD (100/2, v/v); chemical shifts δ are given in ppm. MTX contents of OCM-chitosan-MTX conjugates were determined by a UV spectrophotometer (BECKMAN DUR 640, USA) at 306 nm.

2.4. Measurement of fluorescence spectroscopy

The self-aggregation properties of OCM-chitosan-MTX conjugates and their critical concentrations were determined using fluorescence spectroscopy with pyrene as a fluorescent probe (Amiji, 1995). The pyrene solutions (1.0×10^{-4} mol/L) in methanol were added into a series of test tubes and evaporated under a stream of nitro to remove the solvents. Then, various concentrations of nanoparticle suspension solutions were added to each test tube, and the final concentration of pyrene was 1.0×10^{-6} mol/L, which was nearly equal to the solubility of pyrene in water at 22 °C (Whilhelm et al., 1991). The mixture solutions were sonicated for 30 min in an ultrasonic bath and shaken in an air bath for 1 h at room temperature. Pyrene emission spectra were recorded using fluorescence spectrophotometer (Shimadzu F-4500, Japan). The probe was excited at 333 nm, and the emission spectra were obtained in the range of 350–500 nm at an integration time of 1.0 s. The slit width for excitation and emission were 10 and 2.5 nm, respectively.

2.5. Preparation of self-assembled nanoparticles

OCM-chitosan-MTX nanoparticles were prepared by the dialysis method. Briefly, OCM-chitosan-MTX conjugate (100 mg) was dissolved in 20 mL solution of 0.1 mol/L aqueous hydrochloric acid/dimethylsulfoxide (DMSO) (1/1, v/v), and followed dialyzing (Millipore dialysis tube, molecular weight cut-off 12–14 kDa) against distilled water (500 mL). The medium was replaced every hour for the first 3 h period and every 3 h for the next 24 h until the slight opalescent produced. Then, the dialysate was sonicated using a probe type sonifier (Scintz-IID, China) at 100 W for 2 min (pulse on 2.0 s, pulse off 2.0 s) with three times to form OCM-chitosan-MTX

Table 1
Synthesis of OCM-chitosan-MTX conjugates with different MTX contents.

Samples	OCM-chitosan-MTX-1	OCM-chitosan-MTX-2	OCM-chitosan-MTX-3
OCM-chitosan (g)	0.500	0.500	0.500
NHS-activated MTX (g)	0.500	0.750	1.00
MTX content (w/w %)	10.8	16.2	19.3
MTX DS[a] (mol%)	5.9	8.7	10.6

[a] Degree of substitution of MTX.

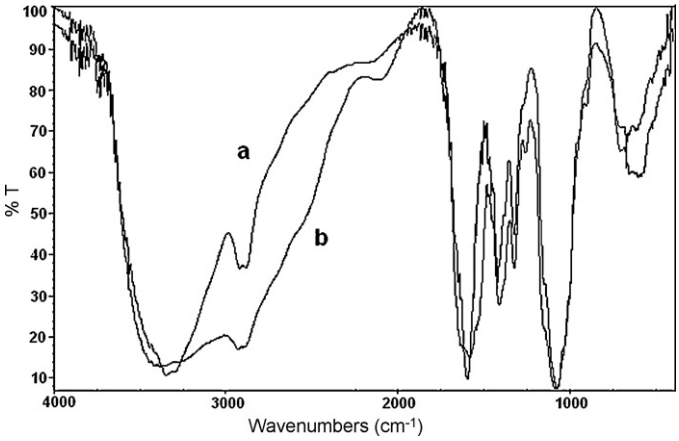

Fig. 1. IR spectra of OCM-chitosan (a) and OCM-chitosan-MTX-3 conjugate (b).

nanoparticles, and subsequently filtered through a filter (0.45 μm, Millipore) to remove dust and impurity.

To observe the morphology of OCM-chitosan-MTX nanoparticles, sample solutions (0.3–0.5 mg/mL) were dropped onto the carbon-coated 300 mesh copper grids. Then, the grids were air-dried and imaged using a transmission electron microscope (Tecnai G^2 20 S-Twin, USA) at an accelerating voltage of 80 kV. The sizes and size distributions of OCM-chitosan-MTX nanoparticles were determined using dynamic laser light scattering (DLLS) with a digital autocorrelator (Brookhaven BI-90 Plus, USA) at a scattering angle of 90°, a wavelength of 633 nm and a temperature of 25 ± 0.1 °C. The zeta potentials of OCM-chitosan-MTX nanoparticles were measured using an electrophoretic light-scattering spectrometer (Brookhaven BI-Zetaplus, USA).

2.6. In vitro drug release study

Drug release behaviors of OCM-chitosan-MTX nanoparticles with different MTX contents were studied by the dynamic dialysis method in PBS buffer solutions (pH 4.0, 7.2 and 9.0). Briefly, the dispersion of OCM-chitosan-MTX nanoparticles in distilled water was placed into Visking dialysis tubing (molecular weight cut-off 12–14 kDa, Millipore, USA) and dialyzed against PBS buffer solution at 37 ± 0.2 °C in an air-bath shaker at 50 rpm. At predefined time intervals, the release media were collected and the fresh release media were added. The release amount of MTX was determined by a UV spectrophotometer (BECKMAN DUR 640, USA) at 306 nm.

3. Results and discussion

To synthesize OCM-chitosan-MTX conjugates, the γ-carboxyl group of MTX was firstly activated by NHS and then chemically coupled with the primary amino group of OCM-chitosan by formation of an amide bond using "zero length" crosslinker of NHS. Since MTX both contains α- and γ-carboxyl groups, we firstly optimized the reaction conditions such as the feed molar ratio of MTX to NHS and the reaction temperature to obtain the selective activation of γ-carboxyl group. In this study, the feed molar ratio (MTX/NHS) of 1:1 and the reaction temperature of 4 °C were finally chosen to prepare NHS-activated MTX. Furthermore, MTX content of OCM-chitosan-MTX conjugate could be controlled by the feed ratio of NHS-activated MTX to OCM-chitosan, which is listed in Table 1.

Fig. 1 shows FTIR spectra of OCM-chitosan and OCM-chitosan-MTX-3 conjugate. The band assignment of OCM-chitosan (Fig. 1A) is as follows (cm^{-1}): 3455 (O—H stretch overlapped with N—H stretch), 2922 and 2879 (C—H stretch), 1650–1550 (C=O stretch of carboxyl methyl group overlapped with amide N—H bend),

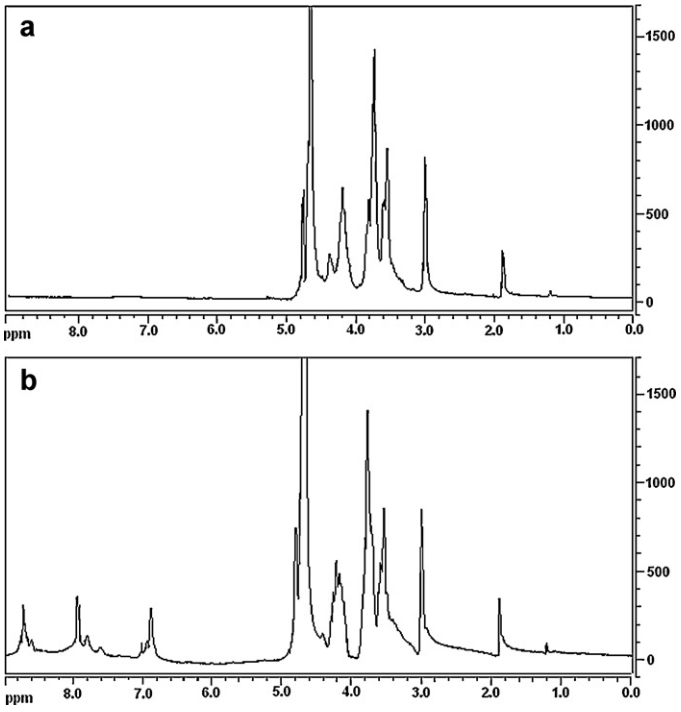

Fig. 2. ^{1}H NMR spectra of OCM-chitosan (a) and OCM-chitosan-MTX-3 conjugate (b).

1409 (C—H bend), 1327 (C—N stretch), 1155 (bridge O stretch), and 1077 (C—O stretch). Compared with OCM-chitosan, the bands of OCM-chitosan-MTX-3 conjugate (Fig. 1B) at 3500–3000 cm^{-1} (O—H stretch overlapped with N—H stretch), 1650–1550 cm^{-1} (C=O stretch overlapped with N—H bend), 1407 cm^{-1} (C—H bend) and 1327 (C—N stretch) obviously increased, which confirmed the formation of amide linkage between the γ-carboxyl group of MTX and the primary amino group of OCM-chitosan.

Fig. 2 shows ^{1}H NMR spectra of OCM-chitosan and OCM-chitosan-MTX-3 conjugate. The proton assignment of OCM-chitosan (Fig. 2A) is as follows (ppm): 1.85 (CH_3, acetamido group of chitosan), 2.97 (*CH*, carbon 2 of glucosamine ring), 3.45 (*CH*, carbon 2 of glucosamine ring with the substituted amino group), 3.6–4.0 (*CH*, carbon 3, 4 and 6 of glucosamine ring), 4.22 (CH_2, carboxymethyl group), 4.38 (*CH*, carbon 5 of glucosamine ring), 4.80 (*CH*, carbon 1 of glucosamine ring). In the spectrum of OCM-chitosan-MTX-3 conjugate (Fig. 2B), the proton signals of MTX moiety in the range of 2.0–5.0 ppm were overlapped with the resonance signals of OCM-chitosan backbone, but the new signals at 6.90, 7.95 and 8.87 ppm were assigned to the protons of benzene and pterin rings of MTX, which indicated that MTX was successfully conjugated to OCM-chitosan.

In aqueous hydrochloric acid (0.1 mol/L), free MTX and OCM-chitosan-MTX conjugates had the same UV absorption characteristics and both showed an absorption peak at around 306 nm, thus UV spectroscopic method (Wang, Han, Li, Wang, & Li, 2007; Wang, Li, Song, & Zhang, 2003; Wang, Liu, Jiang, & Zhang, 2007; Wang, Liu, Weng, & Zhang, 2007) was used to quantitatively measure the MTX contents of OCM-chitosan-MTX conjugates in this study. MTX contents of OCM-chitosan-MTX-1, OCM-chitosan-MTX-2 and OCM-chitosan-MTX-3 were 10.8%, 16.5% and 19.3% respectively, and therefore the degree of substitution (DS) of MTX moiety, defined as the amount of MTX molecules per 100 glucosamine units of chitosan, could be obtained by mathematical conversion and their values were 5.9%, 8.7% and 10.6% (Table 1).

OCM-chitosan-MTX conjugates had the amphiphilic property due to both presence of the hydrophilic polysaccharide backbone of

OCM-chitosan and the hydrophobic MTX grafted moieties. Therefore, they could exhibit self-aggregation behavior, similar to the surfactants in aqueous media. In this study, the fluorescence probe technique with pyrene as a fluorescence probe was used to monitor self-aggregation behavior of OCM-chitosan-MTX conjugates. Pyrene is poorly soluble and a self-quenching agent in a polar environment but strongly emits radiation when micelles or other hydrophobic microdomains are formed in an aqueous solution, as it preferably lies close to (or inside) these hydrophobic microdomains (Amiji, 1995). There are five peaks in the emission spectra of pyrene, and the emission intensity ratio of the first peak (372 nm) and the third peak (385 nm) I_{372}/I_{385} is very sensitive to the polarity of microenvironment. Thus the change in peak I_{372}/I_{385} ratio of pyrene monomer fluorescence could be used to examine self-aggregation behavior of surfactants or polymers in aqueous media (Sui, Song, Chen, & Xu, 2005). The critical micelle concentration, which is the threshold molecular association, can be determined from the change in the intensity ratio (I_{373}/I_{385}) of the pyrene in the presence of polymeric amphiphiles. Fig. 3 shows the changes of the I_{372}/I_{385} values as a function of concentrations of OCM-chitosan-MTX conjugates. The I_{372}/I_{383} values were nearly unchanged at low concentration of OCM-chitosan-MTX, and then followed by a linear decrease with further increasing concentration, and therefore the critical micelle concentration could be determined by the intercept of two straight lines (Lee & Jo, 1998). As shown in Table 2, the critical micelle concentrations of OCM-chitosan-MTX conjugates in aqueous media were in the range of 0.0084–0.0424 mg/mL, which were lower than those of low-molecular-weight surfactants. Table 2 also obviously shows that the critical micelle concentration decreased with MTX content increasing, perhaps due to the increase of the hydrophobicity of inner cores. These results were consistent with other earlier reports (Kwon, Park, Chung, Kwon, & Jeong, 2003; Li et al., 2006).

Three OCM-chitosan-MTX conjugates could form monodispersed nanoparticles by dialysis method combining probe sonication. During dialysis, OCM-chitosan-MTX solution gradually exhibited the slight opalescence, in which the hydrogel particles with irregular morphology were observed by TEM. After dialysis, OCM-chitosan-MTX hydrogel nanoparticles were processed by probe sonication to form small self-assembled nanoparticles. During the probe sonication, the particle size was found to decrease with increasing sonication time, and reached a limiting value after a maximum of 10 min. All samples were sonicated until the limiting size values had been reached.

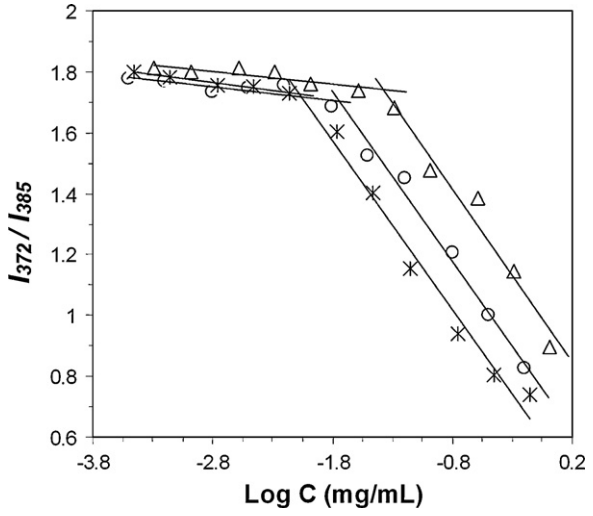

Fig. 3. The relationship of I_{372}/I_{385} from fluorescence spectra of pyrene (1.0×10^{-6} mol/L) with log C of OCM-chitosan-MTX-1 (△), OCM-chitosan-MTX-2 (○) and OCM-chitosan-MTX-3 (✳) conjugates.

Fig. 4 shows the TEM images of OCM-chitosan-MTX nanoparticles. Obviously, OCM-chitosan-MTX-2 and OCM- chitosan-MTX-3 (Fig. 4b and c) nanoparticles had the more spherical shapes and the smaller sizes, compared to OCM- chitosan-MTX-1 (Fig. 4a). Table 2 further shows that the size of OCM-chitosan-MTX nanoparticles determined by DLLS decreased from 363.5 ± 10.4 to 187.2 ± 5.3 nm with MTX content increasing from 10.8% to 19.3% (w/w), which was consistent with the results of other polysaccharide self-assembled nanoparticles that we previously reported (Wang, Liu, Weng, &

Table 2
Characterization of OCM-chitosan-MTX self-assembled nanoparticles.

Samples	CAC[a] ($\times 10^{-2}$ mg/mL)	Diameter[b] (nm)	Polydispersity index[b]	Zeta potential (mV)[c]
OCM-chitosan-MTX-1	4.24	363.5 ± 10.4	0.321 ± 0.082	−8.19 ± 0.98
OCM-chitosan-MTX-2	1.81	231.3 ± 6.5	0.192 ± 0.037	−6.15 ± 0.76
OCM-chitosan-MTX-3	0.84	187.2 ± 5.3	0.156 ± 0.048	−3.08 ± 0.59

[a] Critical aggregation concentration determined from I_{372}/I_{385} data.
[b] The size and size distribution (mean value ± standard deviation) determined by the dynamic laser light scattering with three times.
[c] The zeta potential (mean value ± standard deviation) measured by an electrophoretic light-scattering spectrometer with three times.

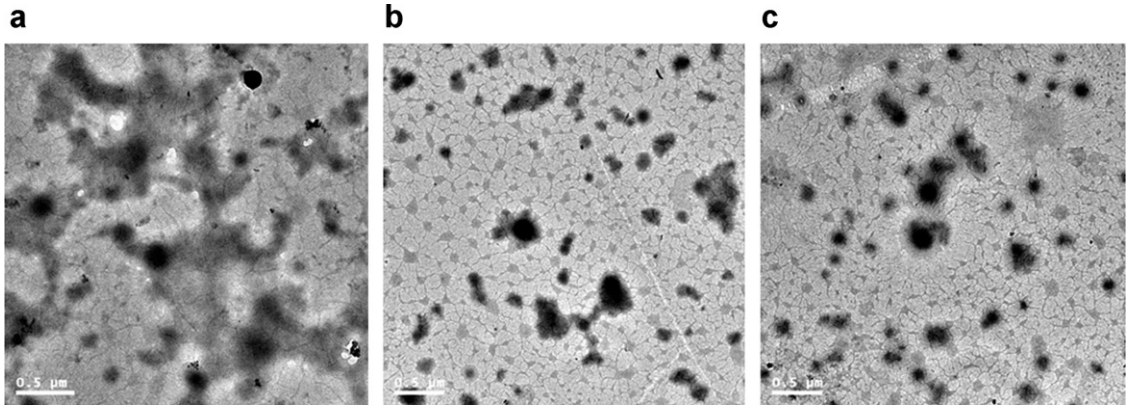

Fig. 4. TEM images of OCM-chitosan-MTX-1 (a), OCM-chitosan-MTX-2 (b) and OCM-chitosan-MTX-3 (c) nanoparticles prepared by the dialysis method combining with probe sonication.

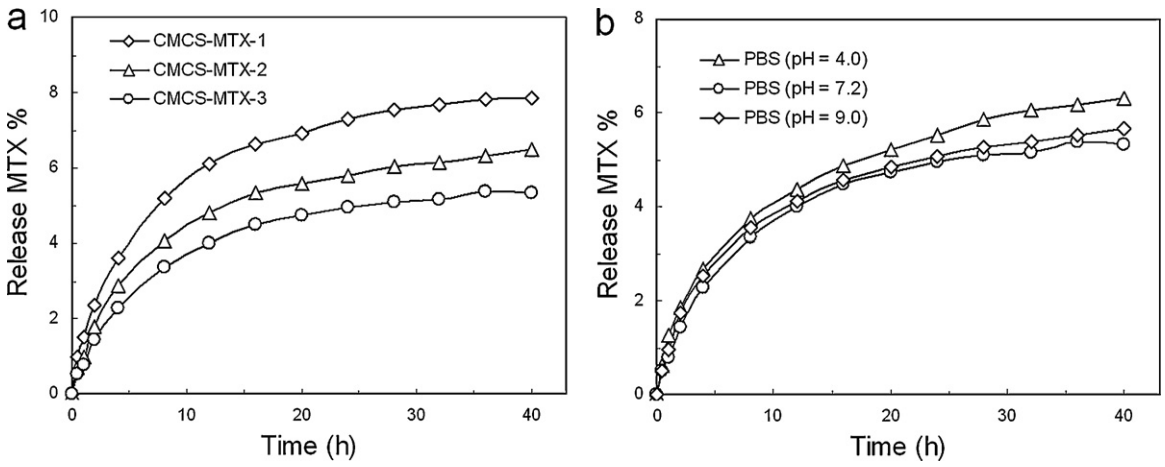

Fig. 5. MTX release curves from OCM-chitosan-MTX nanoparticles at 37 ± 0.2 °C. (a) OCM-chitosan-MTX-1, OCM-chitosan-MTX-2 and OCM-chitosan-MTX-3 nanoparticles in PBS buffer solutions (pH 7.2) and (b) OCM-chitosan-MTX-3 nanoparticles in PBS buffer solutions (pH 4.0, 7.2 and 9.0).

Zhang, 2007). However, the size distribution of OCM-chitosan-MTX nanoparticles increased from 0.156 ± 0.048 to 0.321 ± 0.082 at the same time.

Table 2 also shows that zeta potentials of OCM-chitosan-MTX nanoparticles were negative, e.g., −8.19 ± 0.98, −6.15 ± 0.76 and −3.08 ± 0.59 mV corresponding to OCM-chitosan-MTX-1, OCM-chitosan-MTX-2 and OCM-chitosan-MTX-3, suggesting that the negatively charged carboxymethyl groups in OCM-chitosan-MTX molecules were partially distributed on the surface of nanoparticles due to their hydrophilic property. Evidently, the absolute value of zeta potential decreased with the increase of MTX content. This was perhaps due to that OCM-chitosan-MTX conjugate with higher MTX content formed nanoparticles with the more compact structure and the smaller size, thus resulted the amount of carboxymethyl groups distributed on the surface of nanoparticles decreasing. Furthermore, OCM-chitosan-MTX nanoparticles had evidently the lower absolute values of zeta potentials than other chitosan-based nanoparticles we reported before, such as nanoparticles of cholesterol modified *O*-carboxymethyl chitosan (CCMC), which zeta potentials were −23.19 ± 4.95, −19.92 ± 0.46 and −11.15 ± 1.57 mV, respectively corresponding to CCMC-1, CCMC-2 and CCMC-3 with DS of cholesterol moiety of 6.9%, 9.8 and 12.5% (Wang, Liu, Weng, & Zhang, 2007). It had been reported that neutral nanoparticles would exhibit a decreased rate of macrophage phagocytosis system (MPS) uptake (Alexis, Pridgen, Molnar, & Farokhzad, 2008). Because MPS is the major contributor for the clearance of nanoparticles, the reducing rate of MPS uptake could be considered as the best strategy for prolonging the circulation of the nanoparticles. Therefore, we believed OCM-chitosan-MTX nanoparticles prepared in this study would exhibit the higher stability in blood circulation compared to CCMC nanoparticles (Wang, Liu, Weng, & Zhang, 2007), and related works are in progress now.

OCM-chitosan-MTX conjugates had the similar chemical structure with CCMC (Wang, Liu, Weng, & Zhang, 2007), and therefore the formation mechanism we previously put forward to explain for CCMC nanoparticles also applied to OCM-chitosan-MTX nanoparticles. Briefly, the hydrophobic microdomains are formed by the aggregation of hydrophobic MTX moieties, and OCM-chitosan backbones coil to form the hydrophilic shells outside these hydrophobic microdomains in dialysis process, thus a minimal energy state is attained in aqueous media. Furthermore, the electrostatic attraction between positively charged amino groups and negatively charged carboxyl groups, inter- and/or intramolecular hydrogen bonds among tightly packed polysaccharide backbones will promote the self-assembly of OCM-chitosan-MTX conjugates. In another word, OCM-chitosan-MTX nanoparticle is a non-covalently cross-linked hydrogel structure formed by the hydrophobic association of MTX moieties, and this unique supramolecular structure can be used to encapsulate other hydrophobic drugs, such as angiogenesis inhibitors and multi-drug resistance modulators to obtain multifunctional activities against tumor.

Moreover, it was found that OCM-chitosan-MTX conjugate could not form nanoparticles by the dialysis method when MTX content was less than 10% or more than 20%. Actually, MTX was not only used as the model drug but also as the hydrophobic modified group in this study. Therefore, less or more MTX substitution on the chitosan backbone would not obtain the moderate amphiphilic property, subsequently affected self-assembly behavior of OCM-chitosan-MTX conjugate in aqueous medium.

MTX release behaviors from OCM-chitosan-MTX nanoparticles in PBS buffer solutions were studied by the dynamic dialysis method. Fig. 5(a) shows the cumulative MTX release curves of OCM-chitosan-MTX nanoparticles with different MTX contents in PBS buffer solution (pH 7.2). MTX exhibited significant sustained-release behaviors from all three OCM-chitosan-MTX nanoparticle carriers, about 7.87%, 6.48% and 5.33% MTX released in 40 h corresponding to OCM-chitosan-MTX-1, OCM-chitosan-MTX-2 and OCM-chitosan-MTX-3, respectively. Moreover, MTX release rate evidently decrease with MTX content of OCM-chitosan-MTX conjugate increasing. We believed this was because OCM-chitosan-MTX nanoparticles with the higher MTX content had the more densely packed hydrophobic micro-domains which formed by the aggregation of MTX moieties, and it made more difficult for MTX moieties to exposure to the aqueous media. Thus the hydrolysis rate of amide bonds between MTX moieties and OCM-chitosan accordingly reduced, so the decrease of MTX release rate from OCM-chitosan-MTX nanoparticles was observed.

Fig. 5(b) shows the cumulative MTX release curves of OCM-chitosan-MTX nanoparticles with MTX content of 19.3% in PBS buffers with the pH values of 4.0, 7.2 and 9.0. MTX release rate in PBS buffer (pH 4.0) was slightly higher than in PBS buffers (pH 7.2 and 9.0) but not significant, which was perhaps due to the slightly faster hydrolysis of amide bonds between MTX moieties and polysaccharide backbones at weak acid condition than at the neutral and weak alkaline conditions. Altogether, there was no significant difference among MTX release amounts in PBS buffers with different pH values, about 6.32%, 5.33% and 5.60% MTX released in 40 h corresponding to the pH values of 4.0, 7.2 and 9.0, respectively. The other two OCM-chitosan-MTX nanoparticle samples also showed

the similar release behaviors in different pH PBS buffers. All above results suggested that OCM-chitosan-MTX nanoparticle system had the good *in vitro* stabilities and the potential to be used as a novel carrier for MTX.

4. Conclusions

A novel drug carrier system combining polymeric prodrug with nanotechnology was prepared in this study. MTX, both as the anti-tumor drug and the hydrophobic modified group, was conjugated to OCM-chitosan by amide linkage. OCM-chitosan-MTX conjugate had amphiphilic property and formed nanoparticles in aqueous media by self-assembly. MTX release from OCM-chitosan-MTX nanoparticles significantly prolonged, indicating that this polymeric prodrug nano-system had good *in vitro* stability and had the potential to be used as a novel carrier of MTX.

Acknowledgements

This project was supported by grant from the National Natural Science Foundation of China (No. 30900303), 973 program (2011CB933100) and China Postdoctoral Science Foundation (20100480654).

References

Akiyoshi, K., Yamaguchi, S., & Sunamoto, J. (1991). Self-aggregates of hydrophobic polysaccharide derivatives. *Chemistry Letters*, *7*, 1263–1266.

Alexis, F., Pridge, E., Molnar, L. K., & Fazrokhzaf, O. C. (2008). Factors affecting the clearance and biodistribution of polymeric nanoparticles. *Molecular Pharmaceutics*, *5*(4), 505–515.

Amiji, M. M. (1995). Pyrene fluorescence study of chitosan self-association in aqueous solution. *Carbohydrate Polymers*, *26*(3), 211–213.

Aryal, S., Hu, C. M., & Zhang, L. (2010). Polymer–cisplatin conjugate nanoparticles for acid-responsive drug delivery. *ACS Nano*, *4*(1), 251–258.

Chen, M. M. k., Liu, Y., Yang, W. Z., Li, X. M., Liu, L. R., Zhou, Z. M., et al. (2011). Preparation and characterization of self-assembled nanoparticles of 6-O-cholesterol-modified chitosan for drug delivery. *Carbohydrate Polymers*, *84*, 1244–1251.

David, A., Kopeckova, P., Minko, T., Rubinstein, A., & Kopecek, J. (2004). Design of a multivalent galactoside ligand for selective targeting of HPMA copolymer–doxorubicin conjugates to human colon cancer cells. *European Journal of Cancer*, *40*(1), 148–157.

Dvŏrák, M., Kopečková, P., & Kopeček, J. (1999). High-molecular weight HPMA copolymer adriamycin conjugates. *Journal of Controlled Release*, *60*(2–3), 321–332.

Fang, J., Sawa, T., & Maeda, H. (2003). Factors and mechanism of 'EPR' effect and the enhanced antitumor effects of macromolecular drugs including SMANCS. *Advances in Experimental Medicine and Biology*, *519*, 29–49.

Greish, K., Fang, J., Inutsuka, T., Nagamitsu, A., & Maeda, H. (2003). Macromolecular therapeutics: Advantages and prospects with special emphasis on solid tumour targeting. *Clinical Pharmacokinetics*, *42*(13), 1089– 1105.

Jones, M. C., & Leroux, J. C. (1999). Polymeric micelles—A new generation of colloidal drug carriers. *European Journal of Pharmaceutics and Biopharmaceutics*, *48*, 101–111.

Kumar, M. N. V. R., Muzzarelli, R. A. A., Muzzarelli, C., Sashiwa, H., & Domb, A. J. (2004). Chitosan chemistry and pharmaceutical perspectives. *Chemical Reviews*, *104*, 6017–6084.

Kwon, G. S., & Kataoka, K. (1995). Block copolymer micelles as long-circulating drug vehicles. *Advanced Drug Delivery Reviews*, *16*(2), 295–309.

Kwon, S., Park, J. H., Chung, H., Kwon, I. C., & Jeong, S. Y. (2003). Physicochemical characteristics of self-assembled nanoparticles based on glycol chitosan bearing 5β-cholanic acid. *Langmuir*, *19*(24), 10188–10193.

Lee, K. Y., & Jo, W. H. (1998). Physicochemical characteristics of self-aggregates of hydrophobically modified chitosan. *Langmuir*, *14*(9), 2329–2332.

Li, C. (2002). Poly(L-glutamic acid)-anticancer drug conjugates. *Advanced Drug Delivery Reviews*, *54*(5), 695–713.

Li, Y. Y., Chen, X. G., Yu, L. M., Wang, S. X., Sun, G. Z., & Zhou, H. Y. (2006). Aggregation of hydrophobically modified chitosan in solution and at the air–water interface. *Journal of Applied Polymer Science*, *102*(2), 1968–1973.

Maeda, H. (2001a). SMANCS and polymer-conjugated macromolecular drugs: Advantages in cancer chemotherapy. *Advanced Drug Delivery Reviews*, *46*(1–3), 169–185.

Maeda, H. (2001b). The enhanced permeability and retention (EPR) effect in tumor vasculature: The key role of tumor-selective macromolecular drug targeting. *Advanced Drug Delivery Reviews*, *41*, 189–207.

Matsumura, Y., & Maeda, H. (1986). A new concept for macromolecular therapeutics in cancer chemotherapy: Mechanism of tumoritropic accumulation of proteins and antitumor agent SMANCS. *Cancer Research*, *46*(12), 6387–6392.

Nishiyama, N., & Kataoka, K. (2005). Medical applications of nanotechnology: Polymeric micelles for drug delivery. *Nippon Geka Gakkai Zasshi*, *106*(11), 700–705.

Nogusa, H., Yano, T., Okuno, S., Hamana, H., & Inoue, K. (1995). Synthesis of carboxymethylpullulan–peptide–doxorubicin conjugated and their properties. *Chemical & Pharmaceutical Bulletin*, *43*(11), 1931–1936.

Park, J. H., Cho, Y. W., Son, Y. J., Kim, K., Chung, H., Jeong, S. Y., et al. (2006). Preparation and characterization of self-assembled nanoparticles based on glycol chitosan bearing adriamycin. *Colloid & Polymer Science*, *284*(7), 763–770.

Putnam, D., & Kopeček, J. (1995). Polymer conjugates with anticancer activity. *Advances in Polymer Science*, *122*, 55–123.

Son, Y. J., Jang, J. S., Cho, Y. W., Chung, H., Park, R. W., Kwon, I. C., et al. (2003). Biodistribution and anti-tumor efficacy of doxorubicin loaded glycol-chitosan nanoaggregates by EPR effect. *Journal of Controlled Release*, *91*(1–2), 135–145.

Song, Y., Onishi, H., & Nagai, T. (1992). Synthesis and drug-release characteristics of the conjugates of mitomycinc succinyl-chitosan and carboxymethyl-chitin. *Chemical & Pharmaceutical Bulletin*, *40*(10), 2822–2825.

Sui, W. P., Song, G. L., Chen, G. H., & Xu, G. Y. (2005). Aggregate formation and surface activity property of an amphiphilic derivative of chitosan. *Colloids and Surface A: Physicochemical and Engineering Aspects*, *256*(1), 29–33.

Torchilin, V. P. (2001). Structure and design of polymeric surfactant-based drug delivery systems. *Journal of Controlled Release*, *73*(2–3), 137–172.

Wang, Y. S., Han, Y. L., Li, Y. X., Wang, Y. M., & Li, R. S. (2007). Preparation and in vitro experimental study of methotrexate-lactosyl chitosan conjugate. *Chemical Journal of Chinese Universities*, *28*(6), 1092–1097.

Wang, Y. S., Jiang, Q., Li, R. S., Liu, L. R., Zhang, Q. Q., & Zhao, J. (2008). Self-aggregated nanoparticles of cholesterol-modified *O*-carboxymethyl chitosan as a novel carrier for paclitaxel. *Nanotechnology*, *19*, 145101.

Wang, Y. S., Li, Y. X., Song, N., & Zhang, H. (2003). Preparation and in vitro stability of targeting antitumor drug: Methotrexate-succinyl chitosan conjugate. *Chemical Journal of Chinese Universities*, *24*(11), 2103–2106.

Wang, Y. S., Liu, L. R., Jiang, Q., & Zhang, Q. Q. (2007). Self-aggregated nanoparticles of cholesterol-modified chitosan conjugate as a novel carrier of epirubicin. *European Polymer Journal*, *43*, 43–51.

Wang, Y. S., Liu, L. R., Weng, J., & Zhang, Q. Q. (2007). Preparation and characterization of self-aggregated nanoparticles of cholesterol-modified *O*-carboxymethyl chitosan conjugates. *Carbohydrate Polymers*, *69*, 597–606.

Whilhelm, M., Zhao, C., Wang, Y., Xu, R., Winnik, M. A., Mura, J., et al. (1991). Poly(styrene-ethylene oxide) block copolymer micelle formation in water: A fluorescence probe study. *Macromolecules*, *24*(5), 1033–1044.

Wu, P., He, X. X., Wang, K. M., Tan, W. H., He, C. M., & Deng, M. B. (2009). A novel methotrexate delivery system based on chitosan-methotrexate covalently conjugated nanoparticles. *Journal of Biomedical Nanotechnology*, *5*(5), 557–564.

Yang, X. D., Zhang, Q. Q., Wang, Y. S., Chen, H., Zhang, H. Z., Gao, F. P., et al. (2008). Self-aggregated nanoparticles from methoxy poly(ethylene glycol)-modified chitosan: Synthesis, characterization, aggregation and methotrexate release in vitro. *Colloids and Surfaces B: Biointerfaces*, *61*, 125–131.

Yoo, H. S, Lee, K. H., Oh, J. E., & Park, T. G. (2000). In vitro and in vivo anti-tumor activities of nanoparticles based on doxorubicin-PLGA conjugates. *Journal of Controlled Release*, *68*(3), 419–431.

Yoo, H. S., Oh, J. E., Lee, K. H., & Park, T. G. (1999). Biodegradable nanoparticles containing doxorubicin-PLGA conjugate for sustained release. *Pharmaceutical Research*, *16*(7), 1114–1118.

Zhang, W. Q., Mao, T. Q., Sun, Y. P., He, Y. H., & Wang, W. X. (2000). Preparation and determination of the contents of ferromagnetic methotrexate albumin microspheres. *Journal of Practical Stomatology*, *16*(1), 61–64.